Comparison of airborne lidar measurements with 420 kHz echo-sounder measurements of zooplankton

James H. Churnside and Richard E. Thorne

Airborne lidar has the potential to survey large areas quickly and at a low cost per kilometer along a survey line. For this reason, we investigated the performance of an airborne lidar for surveys of zooplankton. In particular, we compared the lidar returns with echo-sounder measurements of zooplankton in Prince William Sound, Alaska. Data from eight regions of the Sound were compared, and the correlation between the two methods was 0.78. To obtain this level of agreement, a threshold was applied to the lidar return to remove the effects of scattering from phytoplankton.

OCIS codes: 010.3640, 010.4450, 120.0280, 280.3640.

1. Introduction

Large-bodied calanoid copepods of the genus *Neocalanus* are an important component of the ecology of Prince William Sound, Alaska, and have economic consequences through their effect on the salmon fishery. In April and May, these copepods typically form over half of the zooplankton biomass in the Sound.[1] Their large size and high-energy content contribute to their importance as a food source for larger animals in the Sound.[2,3] The timing of natural pink salmon (*Oncorhynchus gorbuscha*) fry entry into salt water is adapted to match that of the migration of *Neocalanus* to the surface in the spring,[4] and survival and early growth rates of pink salmon are dependent on the availability of *Neocalanus* in the spring.[3]

Neocalanus (see the photograph in Fig. 1) are crustaceans with chitin shells. These animals range in length up to several millimeters. *Neocalanus* reproduce over the winter at depths greater than 400 m, and the progeny migrate to the surface to feed on the spring diatom bloom. Diatoms are single-cell algae and are small (50–100 μm) plants, or phytoplankton, whose numbers expand rapidly (bloom) in the spring as soon as there is enough sunlight to support rapid growth. Diatoms tend to form in layers around the depth at which the combination of light level and nutrient concentration are optimum for growth. Zooplankton like *Neocalanus* that feed on diatoms tend to inhabit these layers while feeding.

In 2000, the Prince William Sound Science Center began a series of spring cruises to measure the distribution of zooplankton in the Sound using multiple echo-sounder frequencies and direct net sampling. In particular, these surveys have included an echo sounder at 420 kHz, which is commonly used in zooplankton research.[5–7] While these surveys have been successful, coverage of the Sound is limited by the speed of the ship. The distributions of zooplankton change rapidly, and could be surveyed in much more detail by an effective aerial technique.

Several studies have investigated the detection of fish by lidar, but none have specifically focused on detection of zooplankton. Squire and Krumboltz[8] demonstrated the detection of fish schools with an airborne lidar. More recently, lidar for fish detection has been tested from a ship[9] and in various airborne applications.[10–12] Plankton layers were observed in these tests, but there was no ground truth information available with which to compare the lidar return. To our knowledge this paper is the first quantitative comparison of airborne lidar returns with zooplankton concentrations measured using hydroacoustics and direct sampling.

Our study area was Prince William Sound, Alaska (Fig. 2). Eight regions of the Sound were surveyed by ship on 10–12 May 2002. These same regions were surveyed by air on 14 May. The results show good

J. H. Churnside (james.h.churnside@noaa.gov) is with the National Oceanic and Atmospheric Administration Environmental Technology Laboratory, 325 Broadway, Boulder, Colorado 80305. R. E. Thorne is with Prince William Sound Science Center, P.O. Box 705, Cordova, Alaska 99574.

Received 24 August 2004; revised manuscript received 3 March 2005; accepted 18 April 2005.

0003-6935/05/265504-08$15.00/0

Fig. 1. Photograph of *Neocalanus* copepod.

agreement between the acoustic and lidar results when the lidar data are processed to remove the low-level signals.

2. Lidar System

The National Oceanic and Atmospheric Administration (NOAA) fish lidar is an airborne pulsed lidar,[10] as diagrammed in Fig. 3. The major components are (1) the transmitter laser and beam control optics, (2) the receiver optics and detector, and (3) the data collection and display computer. The receiver telescope and the laser were mounted side by side, and the system was aimed downward through a hole in the bottom of a small twin-engine aircraft (Beechcraft King Air 90), flying at an altitude of 300 m and a speed of $\sim$90 ms^{-1}. To reduce direct surface reflections, the lidar was directed at an angle of 15° from nadir.

The transmitter characteristics were determined by the laser and associated optics. The laser was a neodymium-doped yttrium aluminum garnet (Nd:YAG) laser that was *Q*-switched and frequency doubled. It produced $\sim$100 mJ of 532 nm light in a 12 ns pulse at a repetition rate of 30 Hz. This pulse length produced a measurement volume $\sim$1.3 m long. The laser was linearly polarized, and the beam was diverged by a lens in front of the laser. The divergence was chosen so that the irradiance at the sea surface satisfies the U.S. standard for exposure to laser light in the workplace.[13] This is also safe for marine mammals.[14] The diverged beam was directed by a pair of mirrors so that it was parallel to the axis of the telescope.

The receiver collected, filtered, and detected the light reflected back to the aircraft. It included a 17 cm diameter refracting telescope with a Polaroid filter, which was oriented perpendicular to the polarization

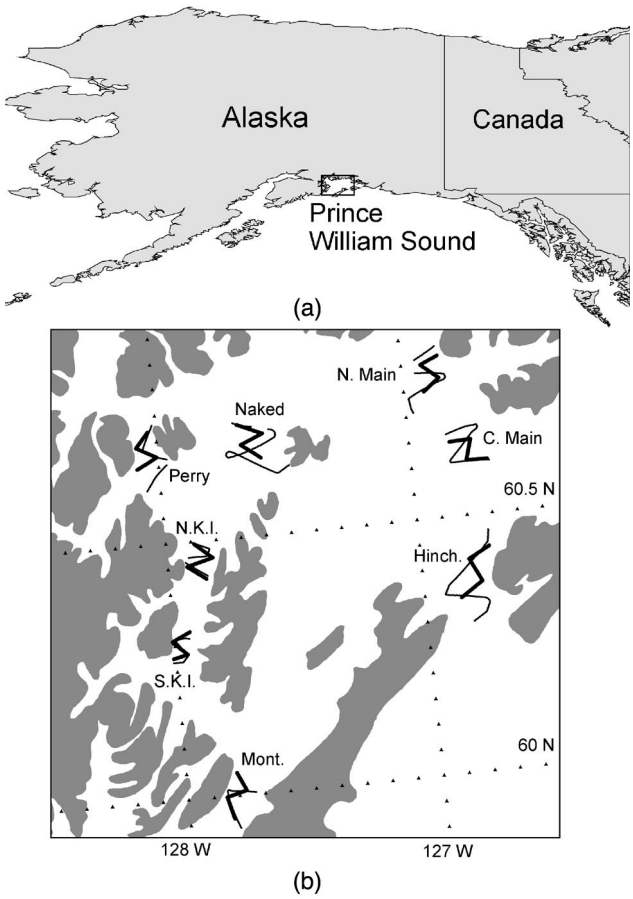

Fig. 2. (a) Map of Alaska and northwestern Canada showing the location of Prince William Sound. (b) Map of Prince William Sound showing locations of acoustic (thick curves) and lidar (thin curves) transects at the Hinchinbrook Entrance (Hinch.), the central main basin (C. Main), the north main basin (N. Main), Naked Island (Naked), Perry Pass (Perry), north Knight Island Passage (N.K.I.), south Knight Island Passage (S.K.I.), and Montague Strait (Mont.).

of the laser. The cross-polarized component was used because it produces the best contrast between fish and smaller scattering particles in the water. This was determined during ship tests of the lidar, where the depolarization of the return from fish was $\sim$30% and the depolarization of the water return was only $\sim$10%.[9] We expect that the depolarization from zooplankton would also be larger than the water background, because they are much larger than the wavelength of light and have a shape that is different from a smooth sphere. The results tend to support this expectation. To reject background light, the light collected by the telescope passed through an interference filter with a bandwidth of 10 nm. Background light was also reduced by an aperture at the focus of the primary lens that matched the field of view of the telescope to the divergence of the transmitted laser beam. The resulting light was incident on a photomultiplier tube (PMT), and the PMT output was logarithmically amplified to increase the dynamic range.

The data collection computer had several func-

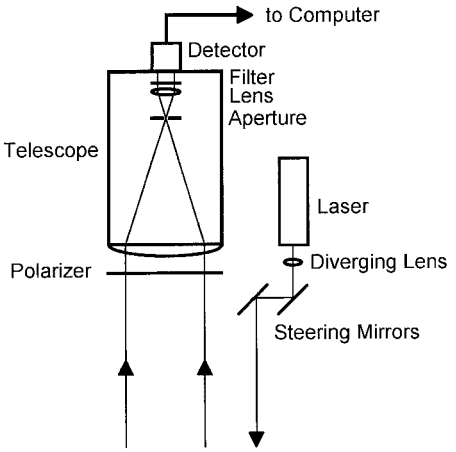

Fig. 3. Schematic diagram of the NOAA fish lidar used in this study.

tions. It digitized and recorded the log-transformed voltage signal with 8 bits of resolution at a rate of 1 GHz. This sample rate corresponds to a depth resolution of 0.11 m. The computer also recorded the aircraft position from the Global Positioning System (GPS), GPS time, the voltage applied to the PMT, and the attitude of the aircraft as measured by tilt sensors and laser gyroscopes on the optical package. The PMT voltage was used to calculate the gain of the tube, which is necessary for calibration. The computer also displayed the data in real time during the flight.

Lidar data processing was performed after the flight, and was done in several steps. These include calculation of the depth-dependent photocathode current, estimation of the excess current at each depth, and application of a threshold to estimate the zooplankton return. The excess current is defined as the photocurrent that is in excess of that which would be expected from a homogeneous distribution of scattering particles.

In the first step, the various component gains were used to calculate the photocathode current for each sample, and the time of each sample was converted to depth in the water column. This step eliminated the effects of changing gain so that all the data were directly comparable. We found the sample corresponding to the surface by identifying the sample with the largest current, and the depth of each sample was found using the 0.11 cm spacing between samples.

The next step in processing was to calculate the excess current for each sample of each return pulse, using a theoretical model of the pulse shape. The backscattered lidar power at depth z can be described by the following equation[10]:

$$S(z) = A[\beta_W + \beta_P(z)] \frac{1}{L^2(z)} \exp(-2\alpha z) + B, \quad (1)$$

where A is a factor that depends on the system parameters and the geometry, β_W is the backscatter coefficient of the water column not including the plankton component, β_P is the backscatter coefficient of the plankton, L is the optical distance from the aircraft to the measurement depth, α is the lidar attenuation coefficient, and B is the background signal level. B, primarily due to skylight reflected from the surface, was measured using the last 100 samples of each pulse, which is after all the laser photons have been absorbed. The standard deviation of these same samples was used as an estimate of the receiver noise, σ_R, for each pulse.

The quantities $A\beta_W$ and α were found for each lidar pulse using Eq. (1) and assuming that (1) β_W does not vary with depth, (2) β_P is zero at a depth of 2 m, and (3) β_P is zero at the maximum penetration depth $z_{\max}$ of each lidar pulse. The depth of 2 m was selected to avoid the effects of scattering from foam and whitecaps that was occasionally observed to extend down to almost this depth. To calculate $z_{\max}$, we first found the depth at which the signal first went below a value of $10\sigma_R$ above B. The median value of 0.8 times this depth over a data segment of 500 pulses ($\sim$1500 m along the flight track) was used as the estimate of $z_{\max}$. A less restrictive definition would produce a greater value for $z_{\max}$, but the signal would be noisier at the greater depths. The three assumptions allowed us to solve the two equations for $S(2)$ and $S(z_{\max})$ for the two parameters required. Visual inspection of the lidar data and of the depth distributions from the acoustic data indicated that the three assumptions were generally satisfied. Note that, if the second and/or third assumption is not true, the background scattering level will be overestimated, producing an estimate of the plankton scattering that is biased low. With these quantities in hand, the excess photocurrent $A\beta_P(z)$ can be found from the measured values of $S(z)$. The factor A was known from laboratory calibration measurements, so we could estimate $\beta_P(z)$ for each pulse. Converting backscatter values into biomass was not possible because measurements have not been done on the polarimetric backscattering characteristics of zooplankton.

We then applied a threshold to the lidar data to remove small values. That is, we set

$$\beta_P(z) = 0 \text{ if } S(z) < TA\beta_W \frac{1}{L^2(z)} \exp(-2\alpha z) + B, \quad (2)$$

where T is the threshold value. A value of $T = 1$ means that all positive estimates of $\beta_P(z)$ were included; negative values are always very small and are assumed to be due to noise. The reason for applying a threshold was the diatom bloom. Our previous qualitative observations suggested that contributions from phytoplankton might have a lower peak scattering strength than those from zooplankton but be more widespread. The phytoplankton return could then dominate the integrated scattering levels, and removing low return power levels might remove the effects of phytoplankton while retaining the scattering from zooplankton. Note that a similar technique

Table 1. Distribution of Zooplankton Samples by Number and Biomass (Percentage and Absolute Values)

Distribution	Small Copepods	Large Copepods	Larvacea	Euphausids	Other
Numerical	87.0%	3.2%	3.2%	1.6%	5.0%
	25,960 m^{-2}	955 m^{-2}	955 m^{-2}	478 m^{-2}	1490 m^{-2}
Biomass	51.1%	35.7%	3.5%	6.5%	3.1%
	10.4 g m^{-2}	7.3 g m^{-2}	0.7 g m^{-2}	1.3 g m^{-2}	0.6 g m^{-2}

is commonly used in acoustics to remove the return from plankton in fish surveys.

3. Acoustic and Sampling Procedures

Acoustic volume backscatter measurements were made at three frequencies: 38 kHz with a BioSonics DT4000 with a 6 deg transducer, 120 kHz with a BioSonics Model 101 with a 7 deg transducer, and 420 kHz with a BioSonics Model 102 with a 6 deg transducer. All were mounted on a 2.4 m towed vehicle and calibrated against standard targets.[15] These three frequencies were chosen because of their common use in surveys of fish,[16] euphausids,[17] and copepods,[5–7] respectively.

The acoustic data were analyzed using standard echo integration techniques.[16,18,19] The DT4000 stores raw digital echo information directly onto a computer hard drive, and it was analyzed using the BioSonics Echo Integration Analyzer Program Version 4.02. The 120 kHz data were recorded on digital audio tape and later processed using the BioSonics Echo Signal Processor (ESP). These frequencies were used only to determine where fish were present.

The 420 kHz data were analyzed in real time using a BioSonics Model 221 ESP. Volume backscattering measurements were made at 2 m depth intervals every 30 s of transect, which corresponded to ~100 m along the lines. Any of these measurements affected by scattering from fish, as determined by a comparison of all three frequencies, was deleted. The large differences in scattering by fish and plankton at the different frequencies make this process effective.[20] Final calibration and acoustic cross-sectional information were added in postprocessing. The acoustic scattering characteristics of large-bodied copepods, pterapods, and euphausids are known[7]; values for the remaining components were estimated by a calculation based on their physical properties.[21,22] For the purposes of this study, the acoustic returns attributed to zooplankton were averaged over depths between 2 and 24 m and over each of the eight areas surveyed.

Zooplankton were sampled at least once in each survey area with a 50 m vertical tow. The net was a 0.5 m diameter ring net with a 0.335 mm mesh.[23] Samples were preserved in the field in 10% formalin. Samples were analyzed to determine both the size and the frequency of the major components.[7] The relative composition of the samples was used to interpret the acoustic data as described above. The absolute numbers from sampling were not compared with the lidar data because the samples were not taken often enough to provide good statistics and because they integrated over more of the water column than the lidar covered.

4. Results

Copepods dominated the zooplankton net catches both numerically and by biomass in all areas. The results are summarized in Table 1. In Table 1 "large" refers to stage IV and *V Neocalanus,* or other copepods of equivalent size. In practice, this typically corresponds to copepods longer than 2 mm.

The acoustic results provide a picture of the overall distribution of zooplankton in the Sound (Table 2). The largest average densities were in the eastern part of the Sound, including the main basin and the Hinchinbrook Entrance. The lowest average densities were in the southwest part of the Sound, including Knight Island Passage and Montague Strait.

For the quantitative comparison of the echosounder and lidar signals, both were averaged over the depth range of 2–24 m. The former represents the minimum depth of the echo sounder, and the latter represents the minimum depth penetration of the lidar for this survey. Overall, 81% of the acoustic energy was within this depth range. The greatest correlation was ~0.78, obtained with a threshold level of $T = 2.75$.

Vertical profiles of energy for the central main basin (Fig. 4) are typical of the similarity between the depth distribution of the acoustic and lidar data. All have been scaled to a value of unity at their respective peaks. In this area of the Sound, 87% of the acoustic energy was within the lidar depth range. The profiles are very similar, with a peak value just below 10 m. The thickness of the layer is ~9 m in the acoustic profile, 8 m in the lidar profile with a threshold of $T = 1$, and 5 m in the lidar profile with $T = 2.75$. The acoustic profile also has a

Table 2. Acoustic and Lidar ($T = 2.75$) Data by Region

Region	Echo Sounder	Lidar
Hinchinbrook Entrance	8.54×10^{-7}	2.60×10^{-7}
Central main basin	5.92×10^{-7}	3.33×10^{-7}
North main basin	6.92×10^{-7}	2.99×10^{-7}
Naked Island	1.94×10^{-7}	1.69×10^{-7}
Perry Pass	3.00×10^{-7}	2.34×10^{-8}
North Knight Island Passage	4.97×10^{-8}	1.27×10^{-8}
South Knight Island Passage	2.31×10^{-8}	4.27×10^{-8}
Montague Strait	1.26×10^{-8}	1.53×10^{-7}

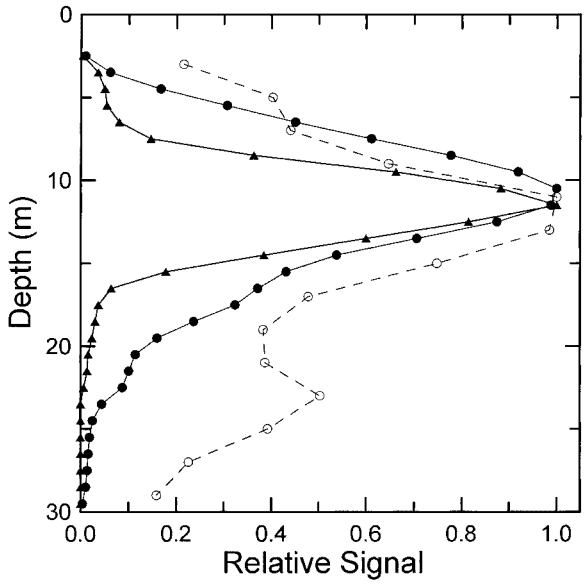

Fig. 4. Acoustic (open circles) and lidar profiles with threshold values of $T = 1$ (filled circles) and $T = 2.75$ (triangles), each normalized by its peak value.

secondary layer at ~23 m that is not present in the lidar data.

When a low threshold ($T = 1$) was applied to the lidar data, the spatial distribution of lidar return in the Sound did not show the same pattern as the acoustic data. In fact, there was a fairly uniform distribution of scattering, except for higher levels in the north part of the main basin, Montague Strait, and north Knight Island Passage, as shown by the circles in Fig. 5. In fact, the correlation between the echo sounder and lidar was only 0.18. The significance of this correlation was $p = 0.67$, where p can be interpreted as the probability that there was actually no correlation.

The application of a higher threshold to the lidar data did affect the correlation (Fig. 6). As the threshold level is increased beyond unity, the correlation level first decreases. This decrease is caused by a decrease in the lidar scattering level in the north main basin region, while the other regions are almost unchanged. A further increase of the threshold level produces an increase in the correlation until it reaches a peak value of around 78% at a value of 2.75. The significance of this result is $p = 0.022$. As the threshold continues to increase, the correlation begins to decrease to a value of ~53%. At threshold levels just above 5, the integrated lidar signal was 0 for one or more of the areas, and these data were not used. It appears that when the threshold is too low, the lidar return contains contributions from particles with lower backscatter cross section, probably phytoplankton and sediments. When the threshold is too high, the return from significant numbers of zooplankton can be removed from the lidar signal.

5. Discussion

In calculating the statistical relationship between the lidar data and the acoustic data with sampling, we have made the implicit assumption that the net samples allow perfect interpretation of the acoustic data, and this is not the case. Earlier studies in Prince William Sound showed a high correlation ($R^2 = 0.77$) between 420 kHz backscatter and catches of large copepods.[20] The tows were made to a depth of 50 m, while the acoustic returns were only integrated to 24 m. The results are valid if the relative distribution of size and type of zooplankton is the same over all depths or if no zooplankton were below 24 m. In our

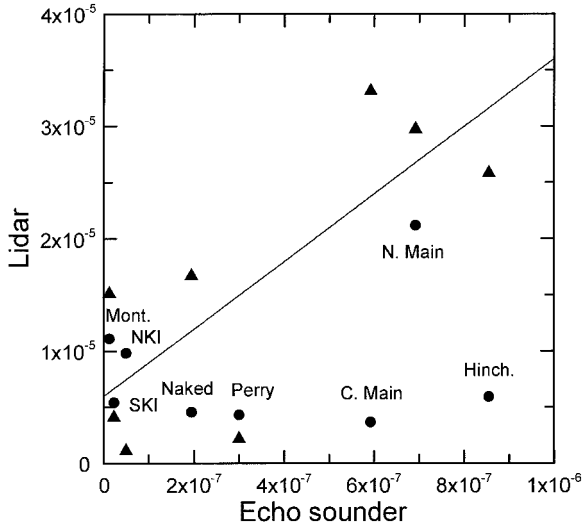

Fig. 5. Scatter plot of lidar data versus echo-sounder data with threshold levels of $T = 1$ (circles) and $T = 2.75$ (triangles). The solid line is the regression of the latter data, which have been multiplied by 100 for clarity of presentation. The circles are labeled with the location of the measurements as in Fig. 2(b); these labels also apply to the triangles with the same echo-sounder values.

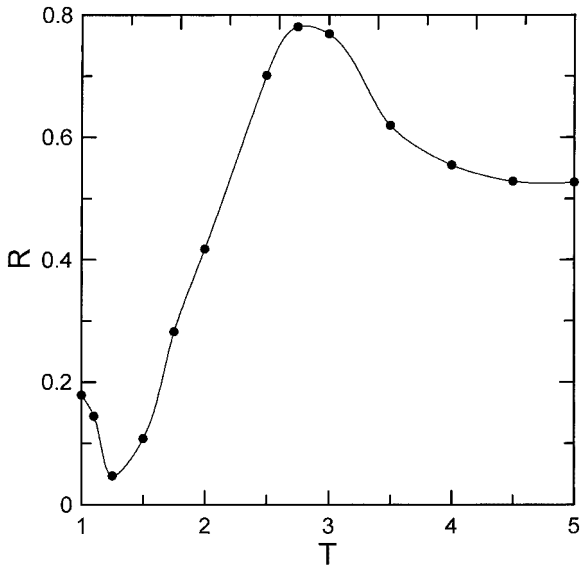

Fig. 6. Correlation coefficient R versus threshold level T for the correlation between the acoustic and the lidar data at the eight locations.

case, 81% of the zooplankton was above 24 m, so the distribution would have to be very different below 24 m to cause a large error in the acoustic results. Tows were made infrequently, and the results were applied to the acoustic returns over a wide area. This will introduce an error if the composition of zooplankton varies over these areas. Certainly, variations occurred over the entire Sound; the variation in the ratio of large to small copepods was ~50% of its mean value for either numbers or biomass. Variations within each region are probably much less. The nets used do not effectively capture euphausids,[7] so the numbers of these may be higher than measured. However, euphausids are typically deeper than 50 m during daylight hours and probably contribute little to the backscattering. Visual identification of life stage can be difficult, although this probably represents a small error in the acoustic interpretation, because animals that look alike probably have similar acoustic scattering characteristics.

Another possible source of error in the absolute numbers is related to the calibration of both the echo sounder and the lidar. Calibration techniques for acoustics have been developed over many years, and frequent calibration of the system with standard targets maintains a value accurate to ± 0.5 dB ($\pm 12\%$).[24] Even large calibration errors in either or both instruments, however, would not change the conclusion of this paper that there is a significant correlation between the two techniques.

One final source of error to be considered is sampling error. The measurements were made 2–4 days apart, and not along the exact same lines. The plankton distributions being measured are patchy and evolving in time in response to the environment. These are the reasons that correlations within each of the measurement areas were not considered; the differences in the times and locations of the measurements are too great to compare anything but the large-scale distributions. The temporal variability is difficult to quantify, but the spatial variability can be obtained either by the acoustic or lidar data. If we look at the correlation distance of the 100 m averages along the acoustic tracks, we find a median value of 230 m. The largest value was ~750 m, observed in the north main basin. The 2–4 days difference in the acoustic and lidar measurements suggest that the plankton would have drifted by many times these distances unless the currents were less than ~ 1 mm s^{-1}.

Despite the sources of error, we observed a significant level of correlation between zooplankton estimates derived from a 420 kHz echo sounder and the backscatter coefficient from lidar with the appropriate threshold applied to the lidar data. This suggests that airborne lidar can be a valuable technique for rapidly surveying zooplankton distributions over a large area under the right conditions.

The first condition is that the plankton in the survey area be dominated by a single type, as in this study. This eliminates the uncertainties introduced by trying to determine how much of the lidar return was from each type of a mixture. This condition can often be met by selecting the location and timing of the survey, which is a common practice in acoustic surveys. Verification that this condition has been met is usually accomplished by direct sampling some portion of the survey area, and this should also be a component of lidar surveys.

The second condition is that most of the plankton be near the surface, where it can be detected by the lidar. This is also a matter of survey design. In the winter, for example, *Neocalanus* would be expected to be at depths greater than 400 m, and they would not be detected by a lidar survey. Later in the spring, they are closer to the surface, and the phytoplankton bloom ends. More research is required to determine the optimal timing for lidar surveys.

The third condition is that the appropriate threshold level be used. If the threshold is too low, significant contributions from phytoplankton are expected, and the zooplankton return would be overestimated. If the threshold is too high, contributions from zooplankton will be ignored, and the return would be underestimated. Some evidence of this effect is seen in the profile data. As in the example of Fig. 4, the layer thickness inferred from the lidar tends to be less when a threshold of 2.75 is applied than that inferred from the echo sounder. This suggests that this threshold may be eliminating the return from zooplankton near the top and bottom of the layer. This would happen if the actual concentration of zooplankton were less near the top and bottom of the layer; it would also happen where measurement volumes near the top and bottom of the layer were only partially filled by the layer, resulting in a smaller average concentration for those range gates.

A fourth condition for obtaining quantitative biomass estimates from the lidar is that the backscatter coefficient be known. While detailed calculation of the backscatter coefficient of copepods is beyond the scope of this work, we can make a rough estimate based on some simplifying assumptions. First, the shell of a copepod is composed of chitin, and we assume that we can represent a copepod as a dielectric sphere of chitin, which has an index of refraction of ~1.56.[25] While a sphere will not depolarize the backscattered light, it is clear from the complexity seen in Fig. 1 that a real copepod will. Therefore, we artificially introduced a depolarization P_x of 0.25. We were unable to find any data on the depolarization of copepods, and this is the measured value for live fish (sardines)[9] as an example. The backscatter coefficient can then be approximated by[26]

$$\beta = P_x N_V \frac{R_F}{2\pi} A_S, \tag{3}$$

where N_V is the volume number density of the particles, R_F is the Fresnel reflectivity for normal incidence, and A_S is the cross section area of a particle.

We can estimate the volume number density by dividing the area number density in Table 1 by the measurement depth range of 22 m. The Fresnel reflectivity of chitin in seawater is $\sim 6.33 \times 10^{-3}$.[25] We can estimate the area for large and small copepods using the number and biomass in Table 1 to get an effective particle diameter, assuming a density about the same as water. Those diameters are 2.44 and 0.92 mm, respectively. For a depolarization of 0.25, the estimated value for both large and small copepods is $\beta = 1.23 \times 10^{-7}\ m^{-1}\ sr^{-1}$, which compares well with the average measured value, $\beta = 1.62 \times 10^{-7}\ m^{-1}\ sr^{-1}$. If we add the other categories of zooplankton in the same way, we get $\beta = 1.40 \times 10^{-7}\ m^{-1}\ sr^{-1}$, which is even closer to the measured value.

The results of this study suggest a combined aerial–surface survey technique for zooplankton. The aircraft would make a large-scale survey to identify regions of greatest zooplankton concentrations. On the basis of the overall distribution, a more limited (in spatial coverage) ship survey would make echosounder measurements to obtain depth distributions and take net samples to obtain species identification, number density, and biomass estimates. These data would be used as calibration data for the lidar to estimate number density and biomass for the rest of the aerial survey.

To obtain more quantitative information from the lidar, independent knowledge of the strength and depolarization of the light backscattered from zooplankton are needed. This same information will allow us to estimate the optimal threshold in advance of future surveys. Sophisticated modeling and comparison with measurements have been done on the acoustic scattering from zooplankton,[27] and a similar effort of modeling and measurements will be required for the lidar case.

This work was partially supported by the Prince William Sound Oil Spill Recovery Institute, Cordova, Alaska. James Wilson of NOAA developed the lidar and installed it in the aircraft. Aircraft support was provided by Airborne Technologies, Inc., of Wasilla, Alaska. The mission was flown by Matt Seebree of Dynamic Aviation.

References

1. R. T. Cooney, K. O. Coyle, E. Stockmar, and C. Stark, "Seasonality in surface-layer net zooplankton communities in Prince William Sound, Alaska," Fish. Oceanogr. **10** (Suppl. 1), 97–109 (2001).
2. R. T. Cooney, "Zooplankton," in *The Gulf of Alaska, Physical Environmental and Biological Resources*, D. W. Hood and S. T. Zimmerman, eds. (Minerals Management Service, U.S. Department of the Interior, 1986), pp. 285–304.
3. T. M. Willette, R. T. Cooney, V. Patrick, D. M. Mason, G. L. Thomas, and D. Scheel, "Ecological processes influencing mortality of juvenile pink salmon (*Onchorynchus gorbuscha*) in Prince William Sound, Alaska," Fish. Oceanogr. **10** (Suppl. 1), 14–41 (2001).
4. R. T. Cooney, J. R. Alen, M. A. Bishop, D. L. Eslinger, T. Kline, B. L. Norcross, C. P. McRoy, J. Milton, J. Olsen, V. Patrick, A. J. Paul, D. Salmon, D. Scheel, G. L. Thomas, S. L. Vaughan, and T. M. Willette, "Ecosystems controls of juvenile pink salmon (*Onchorynchus gorbuscha*) and Pacific herring (*Clupea pallasi*) populations in Prince William Sound, Alaska," Fish. Oceanogr. **10** (Suppl. 1), 1–13 (2001).
5. M. C. Benfield, P. H. Wiebe, T. K. Stanton, C. S. Davis, S. M. Gallager, and C. H. Greene, "Estimating the spatial distribution of zooplankton biomass by combining video plankton recorder and single-frequency acoustic data," Deep-Sea Res. II **45,** 1175–1199 (1998).
6. C. H. Greene, P. H. Wiebe, P. Pelkie, M. C. Benfield, and J. M. Popp, "Three-dimensional acoustic visualization of zooplankton patchiness," Deep-Sea Res. II **45,** 1201–1217 (1998).
7. J. Kirsch, G. L. Thomas, and R. T. Cooney, "Acoustic estimates of zooplankton distributions in Prince William Sound, spring 1996," Fish. Res. **47,** 245–260 (2000).
8. J. L. Squire, Jr., and H. Krumboltz, "Profiling pelagic fish schools using airborne optical lasers and other remote sensing techniques," Mar. Technol. Soc. J. **15,** 27–31 (1981).
9. J. H. Churnside, J. J. Wilson, and V. V. Tatarskii, "Lidar profiles of fish schools," Appl. Opt. **36,** 6011–6020 (1997).
10. J. H. Churnside, J. J. Wilson, and V. V. Tatarskii, "Airborne lidar for fisheries applications," Opt. Eng. **40,** 406–414 (2001).
11. J. H. Churnside, D. A. Demer, and B. Mahmoudi, "A comparison of lidar and echosounder measurements of fish schools in the Gulf of Mexico," ICES J. Mar. Sci. **60,** 147–154 (2003).
12. E. D. Brown, J. H. Churnside, R. L. Collins, T. Veenstra, J. J. Wilson, and K. Abnett, "Remote sensing of capelin and other biological features in the north Pacific using lidar and video technology," ICES J. Mar. Sci. **59,** 1120–1130 (2002).
13. American National Standards Institute, *Safe Use of Lasers, Standard Z-136.1* (Laser Institute of America, 1993), p. 120.
14. H. M. Zorn, J. H. Churnside, and C. W. Oliver, "Laser safety thresholds for cetaceans and pinnipeds," Mar. Mammal Sci. **16,** 186–200 (2000).
15. K. G. Foote, H. P. Knudsen, G. Vestnes, D. N. MacLennan, and E. G. Simmonds, "Calibration of acoustic instruments for fish density estimation: a practical guide," ICES Coop. Res. Rep. 144 (International Council for the Exploration of the Seas, 1987).
16. D. N. MacLennan and E. J. Simmonds, *Fisheries Acoustics* (Chapman & Hall, 1992).
17. D. E. McGehee, R. L. Driscoll, and L. V. Martin Traykovski, "Effects of orientation on acoustic scattering from Antarctic krill at 120 kHz," Deep-Sea Res. II **45,** 1273–1294 (1998).
18. R. E. Thorne, "Hydroacoustics," in *Fisheries Techniques*, L. Nielson and D. Johnson, eds. (American Fisheries Society, 1983).
19. R. E. Thorne, "Assessment of population abundance by echo integration," in *Proceedings of the Symposium on Assessment of Micronekton,* Biol. Ocean. J. **2,** 253–262 (1983).
20. R. E. Thorne and G. L. Thomas, "Monitoring the juvenile pink salmon food supply and predators in Prince William Sound," in *Workshop on Factors Affecting Production of Juvenile Salmon: Comparative Studies on Juvenile Salmon Ecology Between the East and West North Pacific Ocean*, Tech. Rep. 2, R. Beamish, Y. Ishida, V. Karpenko, P. Livingston, and K. Meyers, eds. (North Pacific Anadromous Fish Commission, 2001).
21. D. V. Holliday and R. E. Pieper, "Volume scattering strengths and zooplankton distributions at acoustic frequencies between 0.5 and 3 MHz," J. Acoust. Soc. Am. **67,** 135–146 (1995).
22. P. H. Wiebe, T. K. Stanton, M. C. Benfield, D. G. Mountain, and C. H. Greene, "High-frequency acoustic volume backscattering in the Georges Bank coastal region and its interpretation using scattering models," IEEE J. Ocean. Eng. **22,** 445–464 (1997).

23. R. T. Cooney, T. M. Willette, S. Sharr, D. Sharp, and J. Olsen, "The effect of climate on North Pacific pink salmon (*Onchorynchus gorbuscha*) production: examining some details of a natural experiment," Can. Spec: Publ. Fish. Aquat. Sci. **121,** 475–482 (1995).
24. R. E. Thorne, "Acoustic surveying of pelagic fish in shallow water," *Proceedings of the IEEE Geoscience and Remote Sensing Symposium* (IEEE Press, 2004).
25. M. F. Land, "The physics and biology of animal reflectors," Prog. Biophys. Mol. Biol. **24,** 75–106 (1972).
26. K. S. Shifrin, *Physical Properties of Ocean Water* (American Institute of Physics, 1988), p. 119 ff.
27. A. C. Lavery, T. K. Stanton, D. E. McGehee, and D. Chu, "Three-dimensional modeling of acoustic backscattering from fluid-like zooplankton," J. Acoust. Soc. Am. **111,** 1197–1210 (2002).